Boundary-element modeling of free subduction beneath an overriding plate: role of the subduction interface and partitioning of viscous dissipation

Gianluca Gerardi[1], Neil M. Ribe[1], Paul J. Tackley[2]

[1]Lab FAST, Univ Paris-Sud/CNRS, Orsay (France)
[2]Institute of Geophysics, ETH, Zurich (Switzerland)

EGU General Assembly
Vienna, 08-13 April 2018

This project has received funding from the European Union's Horizon 2020 research and innovation programme under the Marie Sklodowska-Curie grant agreement No 642029 - ITN CREEP.

Introduction

Modeling of subducting plate (SP)/overriding plate (OP) interaction along the subduction interface (SI)

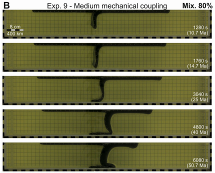

Duarte *et al.* (2013)

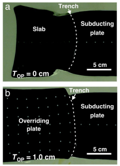

Meyer *et al.* (2013)

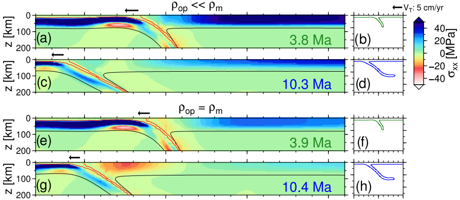

Holt *et al.* (2015)

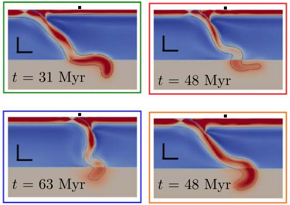

Garel *et al.* (2014)

Critical aspects to address

1. Mechanical role of the subduction interface
   - Influence on SP convergence rate
2. Partitioning of viscous dissipation
   - Influence on globale-scale mantle convection models

Model setup

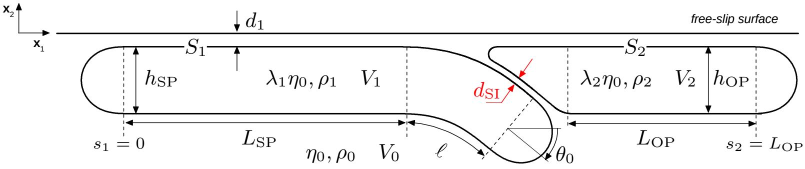

- Purely viscous plate;
- Infinitely deep ambient fluid;
- Buoyancy-driven subduction;
- Stokes equations of motion;
- Boundary-element method.

KEY DIMENSIONLESS PARAMETERS

$\boldsymbol{R_{\min}}$ **= min. radius of curvature**

$\boldsymbol{\ell_b}$ **= bending length= $\boldsymbol{\ell + \ell_{fb}}$**

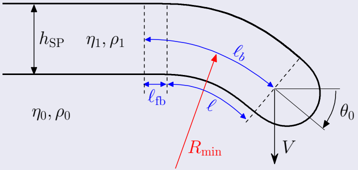

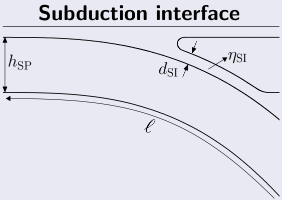

$$\mathrm{St} \equiv \frac{\eta_1}{\eta_0}\left(\frac{h_{SP}}{\ell_b}\right)^3 \rightarrow \text{Plate flexural stiffness}$$

$$\gamma \equiv \frac{\eta_{SI}}{\eta_0}\left(\frac{h_{SP}}{d_{SI}}\right) \rightarrow \text{Interface strength}$$

Instantaneous convergence rate: V_{Conv}

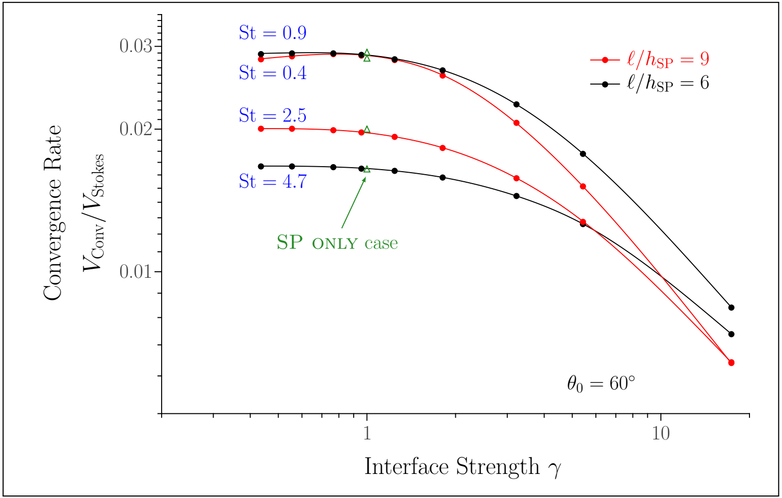

Features

Global scaling law

$$\frac{V_{\mathrm{Conv}}}{V_{\mathrm{Stokes}}} = \mathrm{fct}\Big(\underbrace{\theta_0, \frac{\ell}{h_{\mathrm{SP}}}}_{\text{geometry}}, \mathrm{St}, \gamma\Big)$$

$\boldsymbol{V_{\mathrm{Conv}}}$ decreases for:

- Stiffer SP
- Stronger SI

Fixed slab geometry:

$$\frac{V_{\mathrm{Conv}}}{V_{\mathrm{Stokes}}} = \mathrm{fct}\left(\lambda_1, \gamma\right)$$

$\Rightarrow$ Assuming a range of viscosity ratios (λ_1), constrain γ using observed V_{Conv}

Case study: central Aleutian subduction zone

Geometry and V_{Conv} from Lallemand et al. (2005)

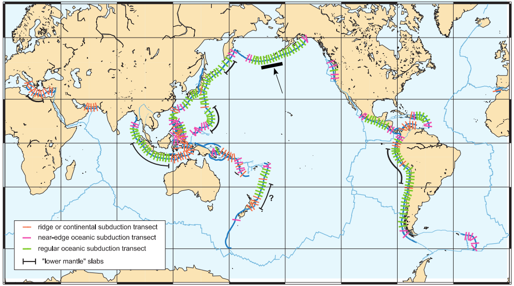

- Quasi-2D subduction
- Slab far from the 660 km discontinuity

Inferred subduction interface strength

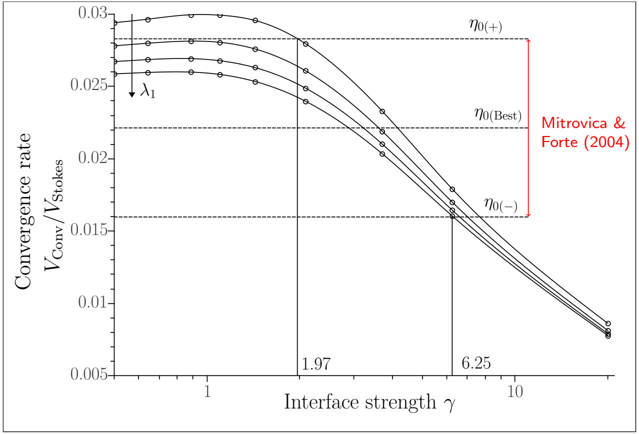

For $\lambda_1 \in [250 - 450] \Rightarrow \gamma \in [2 - 6]$

$d_{\mathrm{SI}}/h_{\mathrm{SP}} \approx 0.07 \Rightarrow \eta_{\mathrm{SI}}/\eta_0 \approx 0.3$

Rates of viscous dissipation of energy

Energy dissipation

Is mantle convection primarily resisted by the deformation occurring at subduction zones (e.g. Conrad&Hager, 1999) ?

Balance of mechanical energy

$$D_{\mathrm{Total}} = D_{\mathrm{SI}} + D_{\mathrm{SP}} + D_{\mathrm{OP}} + D_{\mathrm{M}}$$

Rate of release of gravitational energy

$$D_{\mathrm{Total}} = \Delta\rho_1 g \int_{S_1} u_i(\mathbf{y}) n_i(\mathbf{y}) y_j \, dl(\mathbf{y})$$

Rate of viscous dissipation within the subduction interface

$$D_{\mathrm{SI}} = 2\eta_{\mathrm{SI}} \int_{A_{\mathrm{SI}}} e_{ij} e_{ij} \, dA_{\mathrm{SI}}$$

Rate of viscous dissipation within the plates
from thin-sheet theory *(Ribe, 2001)*:

$$D_{\mathrm{SP/OP}} = \int_{L_s} \left[\underbrace{4\eta_i h_i \Delta^2(s_i)}_{\text{stretching}} + \underbrace{\frac{1}{3}\eta_i h_i^3 \dot{K}^2}_{\text{bending}} \right] ds_i$$

$\Delta =$ Midsurface stretching rate
$\dot{K} =$ Rate of change of midsurface curvature

$i = 1$ or 2 for SP and OP properties, respectively

Dissipation ratio

$$R = \frac{D_{\mathrm{SP}} + D_{\mathrm{OP}} + D_{\mathrm{SI}}}{D_{\mathrm{Total}}} = \frac{D_{\mathrm{BL}}}{D_{\mathrm{Total}}}$$

SP+OP case: time dependent solutions

$\lambda_1 = \lambda_2 = 250$

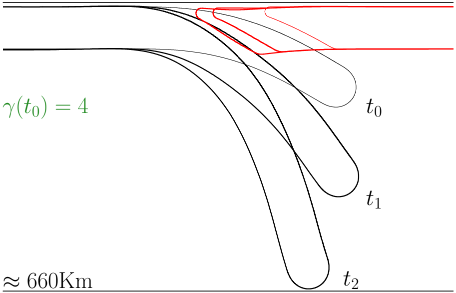

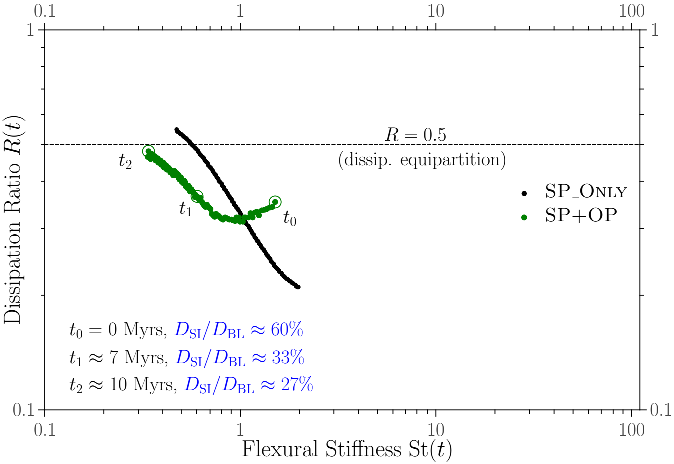

SP+OP case: time dependent solutions

$\lambda_1 = \lambda_2 = 2500$

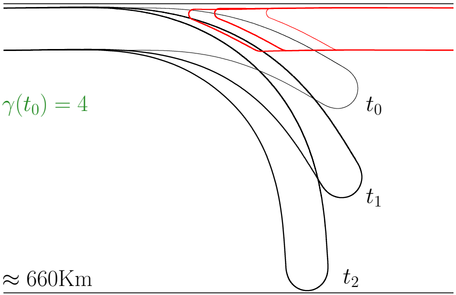

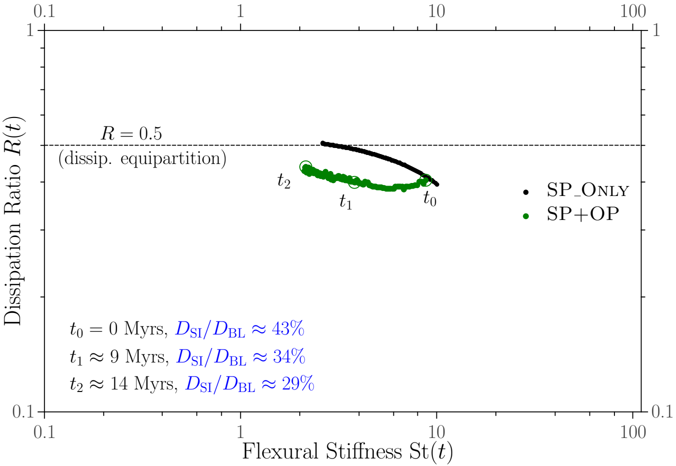

For realistic time-dependent solutions, $R \in [0.3 - 0.5]$

Steady-state analysis of thermal convection (e.g. Turcotte & Schubert, 2014)

Geometry of the convecting cell:

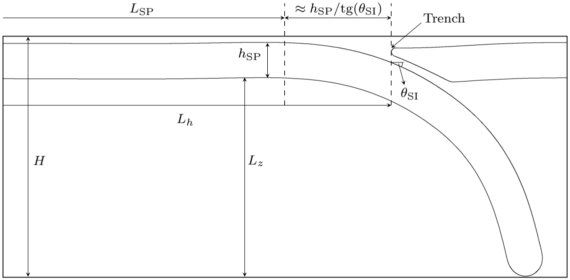

Note: $h_{\mathrm{SP}}=$ SP's thickness as it enters into the subduction zone

Assumptions:

- No heat sources; well-mixed mantle at temperature T_m
- Temperature gradient across the SP: $\Delta T = T_m - T_{\mathrm{Surf}}$

Total surface heat flow $\rightarrow Q = 2K\Delta T\left[U_{\mathrm{SP}}L_h/(\pi\kappa)\right]^{1/2}$

Mass conservation $\rightarrow U_{\mathrm{SP}}/L_h \sim V_{\mathrm{Sink}}/L_z$

Nusselt number (Q/Q_c)

$$\mathrm{Nu} \sim \left(\frac{H^2 V_{\mathrm{Sink}}}{\kappa L_z}\right)^{1/2}$$

Energy balance

$$V_{\mathrm{Sink}} \sim \frac{h_{\mathrm{SP}}\ell g \Delta\rho_1}{\eta_0 \mathrm{f}_2(\theta)\,(1 + C_{\mathrm{R}})}$$

$\mathrm{f}_2(\theta)$ $\downarrow$ Geometrical effect; C_{R} $\searrow$ $D_{\mathrm{BL}}/D_{\mathrm{M}}$

WEAK BL ($C_{\mathrm{R}} \rightarrow 0$)

Thermal thickening

$$\frac{h_{\mathrm{SP}}}{H} \sim \left(\frac{L_z \mathrm{f}_2(\theta)}{\ell \mathrm{Ra}_{\mathrm{m}}}\right)^{1/3}. \quad \mathrm{Ra}_{\mathrm{m}} \equiv \frac{H^3 g \Delta\rho_1}{\kappa\eta_0}$$

$$\mathrm{Nu} \sim \mathrm{Ra}_{\mathrm{m}}{}^{1/3}\left(\frac{\ell}{L_z \mathrm{f}_2(\theta)}\right)^{1/3}$$

Steady-state analysis of thermal convection (e.g. Turcotte & Schubert, 2014)

Conrad&Hager (1999) approach: $\mathbf{Ra_{SP}} \equiv \dfrac{\boldsymbol{\ell_b^3 g \Delta \rho_1}}{\boldsymbol{\kappa \eta_1}}$, $\mathbf{Ra_{SI}} \equiv \dfrac{\boldsymbol{d_{SI}^3 g \Delta \rho_1}}{\boldsymbol{\kappa \eta_{SI}}}$

$D_{\mathrm{SP/SI}} \gg 1 \Rightarrow \mathrm{Ra}_{\mathrm{SP/SI}} \ll 1$

$$V_{\mathrm{Sink}} \sim \mathrm{Ra_m} \frac{h_{\mathrm{SP}} \ell \kappa}{\mathrm{f_2}(\theta) H^3} \left[1 + \underbrace{\frac{\mathrm{Ra_m}}{\mathrm{Ra_{SP}}} \left(\frac{h_{\mathrm{SP}}}{H} \right)^3 \mathrm{F}(\theta)}_{\text{SP bending}} + \underbrace{\frac{\mathrm{Ra_m}}{\mathrm{Ra_{SI}}} \left(\frac{h_{\mathrm{SP}}}{H} \right) \left(\frac{d_{\mathrm{SI}}^2}{H^2 \sin(\theta_{\mathrm{SI}}) \mathrm{f_2}(\theta)} \right) \left(\frac{V_{\mathrm{Conv}}}{V_{\mathrm{Sink}}} \right)^2}_{\text{SI shearing}} \right]^{-1}$$

Steady-state analysis of thermal convection (e.g. Turcotte & Schubert, 2014)

Conrad&Hager (1999) approach: $\mathbf{Ra_{SP}} \equiv \dfrac{\boldsymbol{\ell_b^3 g \Delta\rho_1}}{\boldsymbol{\kappa\eta_1}}$, $\mathbf{Ra_{SI}} \equiv \dfrac{\boldsymbol{d_{SI}^3 g \Delta\rho_1}}{\boldsymbol{\kappa\eta_{SI}}}$

$D_{\mathrm{SP/SI}} \gg 1 \Rightarrow \mathrm{Ra}_{\mathrm{SP/SI}} \ll 1$

$$V_{\mathrm{Sink}} \sim \mathrm{Ra_m} \frac{h_{\mathrm{SP}}\ell\kappa}{\mathrm{f}_2(\theta)H^3}\left[1 + \underbrace{\frac{\mathrm{Ra_m}}{\mathrm{Ra_{SP}}}\left(\frac{h_{\mathrm{SP}}}{H}\right)^3 \mathrm{F}(\theta)}_{\text{SP bending}} + \underbrace{\cancel{\frac{\mathrm{Ra_m}}{\mathrm{Ra_{SI}}}\left(\frac{h_{\mathrm{SP}}}{H}\right)\left(\frac{d_{\mathrm{SI}}^2}{H^2\sin(\theta_{\mathrm{SI}})\mathrm{f}_2(\theta)}\right)\left(\frac{V_{\mathrm{Conv}}}{V_{\mathrm{Sink}}}\right)^2}}_{\text{SI shearing}}\right]^{-1}$$

STRONG BL $(C_{\mathrm{R}} \neq 0, D_{\mathrm{SI}} = 0)$

Thermal thickening

$$\frac{h_{\mathrm{SP}}}{H} \sim \left(\frac{\mathrm{Ra_{SP}}}{\mathrm{Ra_m}} \frac{L_z \mathrm{f}_2(\theta)}{\mathrm{Ra_{SP}}\ell - \mathrm{f}_1(\theta)L_z}\right)^{1/3}$$

$$\mathrm{Nu} \sim \mathrm{Ra_m}^{1/3}\left(\frac{\ell}{L_z \mathrm{f}_2(\theta)} - \frac{\mathrm{F}(\theta)}{\mathrm{Ra_{SP}}}\right)^{1/3}$$

Steady-state analysis of thermal convection (e.g. Turcotte & Schubert, 2014)

Conrad&Hager (1999) approach: $\mathbf{Ra_{SP}} \equiv \dfrac{\ell_b^3 g \Delta\rho_1}{\kappa\eta_1}$, $\mathbf{Ra_{SI}} \equiv \dfrac{d_{SI}^3 g\Delta\rho_1}{\kappa\eta_{SI}}$

$D_{SP/SI} \gg 1 \Rightarrow \mathrm{Ra}_{SP/SI} \ll 1$

$$V_{\mathrm{Sink}} \sim \mathrm{Ra_m}\frac{h_{\mathrm{SP}}\ell\kappa}{\mathrm{f}_2(\theta)H^3}\left[1+\underbrace{\frac{\mathrm{Ra_m}}{\mathrm{Ra_{SP}}}\left(\frac{h_{\mathrm{SP}}}{H}\right)^3\mathrm{F}(\theta)}_{\text{SP bending}}+\underbrace{\cancel{\frac{\mathrm{Ra_m}}{\mathrm{Ra_{SI}}}\left(\frac{h_{\mathrm{SP}}}{H}\right)\left(\frac{d_{\mathrm{SI}}^2}{H^2\sin(\theta_{\mathrm{SI}})\mathrm{f}_2(\theta)}\right)\left(\frac{V_{\mathrm{Conv}}}{V_{\mathrm{Sink}}}\right)^2}}_{\text{SI shearing}}\right]^{-1}$$

Strong BL $(C_{\mathrm{R}} \neq 0, D_{\mathrm{SI}} = 0)$

Thermal thickening

$$\frac{h_{\mathrm{SP}}}{H} \sim \left(\frac{\mathrm{Ra_{SP}}}{\mathrm{Ra_m}}\frac{L_z\mathrm{f}_2(\theta)}{\mathrm{Ra_{SP}}\ell - \mathrm{f}_1(\theta)L_z}\right)^{1/3}$$

$$\mathrm{Nu} \sim \mathrm{Ra_m}^{1/3}\left(\frac{\ell}{L_z\mathrm{f}_2(\theta)} - \frac{\mathrm{F}(\theta)}{\mathrm{Ra_{SP}}}\right)^{1/3}$$

Domain of validity

$$\mathrm{Ra_{SPcr}} \rightarrow \frac{\mathrm{f}_1(\theta)L_z}{\ell} \Rightarrow h_{\mathrm{SP}} \rightarrow \infty \quad \mathrm{Nu} \rightarrow 0$$

Upper mantle convection

$\mathrm{Ra_m} \in [10^5 - 10^6]$, $H/h_{\mathrm{SP}} = 6.7$

$R_{\mathrm{cr}} \approx 0.87$

BEM numerical solutions $(\lambda_1 \in [250 - 2500])$

$R \in [0.3 - 0.5]$

D_{SP} evaluation

$D_{\mathrm{SP}} \sim L^{-3} \to L=$ length scale describing the bending response of the SP

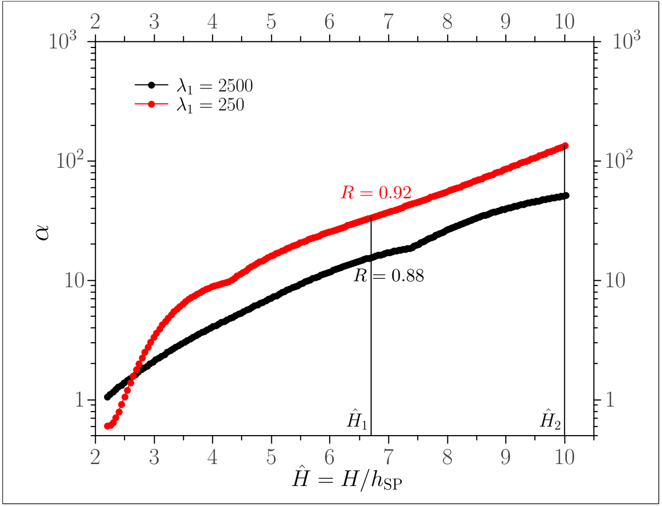

Overestimation

- $\alpha = \dfrac{D_{\mathrm{SP}}|_{R_{\min}}}{D_{\mathrm{SP}}|_{\ell_b}} = \left(\dfrac{\ell_b}{R_{\min}}\right)^3$
- D_{SP} depends strongly on L and H
- $h_{\mathrm{SP}} \approx 100$ km, $H \approx 1000$ km and $R_{\min} \approx 400$ km
  $\Rightarrow \alpha \approx 10^2 \quad (R > 0.9)$
- Conrad&Hager (1999): $H \approx 2500$ km and $R_{\min} \approx 200$ km
  $\Rightarrow \alpha > 10^2$

Conclusions

Subduction zone interface

- The strength of the interface and the flexural stiffness of the SP strongly affect V_{Conv};
- The comparison of the predicted V_{Conv} of our numerical simulations with the observed values given by Lallemand et al. (2005) regarding the central Aleutian slab suggests $\gamma \in [2-6]$.

Energetics of subduction

- When subduction starts D_{SI} can give the highest contribution to the the deformation of the BL (60% for $\lambda_1 = 250$). As subduction proceeds, its importance diminishes;
- For viscosity ratios $\in [250-2500]$ and $H/h_{\mathrm{SP}} \in [2-7]$, $R = D_{\mathrm{BL}}/D_{\mathrm{M}} \in [0.3-0.5]$.

Global-scale mantle convection models

- Combining our numerical solutions with the steady-state boundary layer analysis of upper mantle convection we find $\mathrm{Nu} \sim \mathrm{Ra_m}^{1/3} f(\mathrm{Ra_{SP}})^{1/3}$;
- A wrong length scale can lead to a strong overestimation of D_{SP} which, in turn, increases as we consider a thicker convecting cell.

ExtraSlide: BEM formulation

Boundary-Integral representation

$$\frac{\Delta\rho_1}{\eta_0}\int_{S_1}(\boldsymbol{g}\cdot\boldsymbol{y})\,\boldsymbol{n}(\boldsymbol{y})\cdot\boldsymbol{J}(\boldsymbol{y}-\boldsymbol{x})dl(\boldsymbol{y})+\frac{\Delta\rho_2}{\eta_0}\int_{S_2}(\boldsymbol{g}\cdot\boldsymbol{y})\,\boldsymbol{n}(\boldsymbol{y})\cdot\boldsymbol{J}(\boldsymbol{y}-\boldsymbol{x})dl(\boldsymbol{y})+$$
$$+(1-\lambda_1)\int_{S_1}\boldsymbol{u}^{(1)}(\boldsymbol{y})\cdot\boldsymbol{K}(\boldsymbol{y}-\boldsymbol{x})\cdot\boldsymbol{n}(\boldsymbol{y})+(1-\lambda_2)\int_{S_2}\boldsymbol{u}^{(2)}(\boldsymbol{y})\cdot\boldsymbol{K}(\boldsymbol{y}-\boldsymbol{x})\cdot\boldsymbol{n}(\boldsymbol{y})=$$
$$=\left\{\begin{array}{ll}(1+\lambda_1)/2\ \boldsymbol{u}^{(1)}(\boldsymbol{x}), & \text{if } \boldsymbol{x}\in S_1\\ (1+\lambda_2)/2\ \boldsymbol{u}^{(2)}(\boldsymbol{x}), & \text{if } \boldsymbol{x}\in S_2\end{array}\right\}$$

Nondimensionalization

$(\hat{\boldsymbol{x}},\hat{\boldsymbol{y}})=h_1^{-1}(\boldsymbol{x},\boldsymbol{y})$ $\qquad \hat{\boldsymbol{u}}=\boldsymbol{u}\dfrac{\eta_0}{h_1^2 g\Delta\rho_1}$ $\qquad \hat{t}=t\dfrac{h_1 g\Delta\rho_1}{\eta_0}$

ExtraSlide: Bending length definition

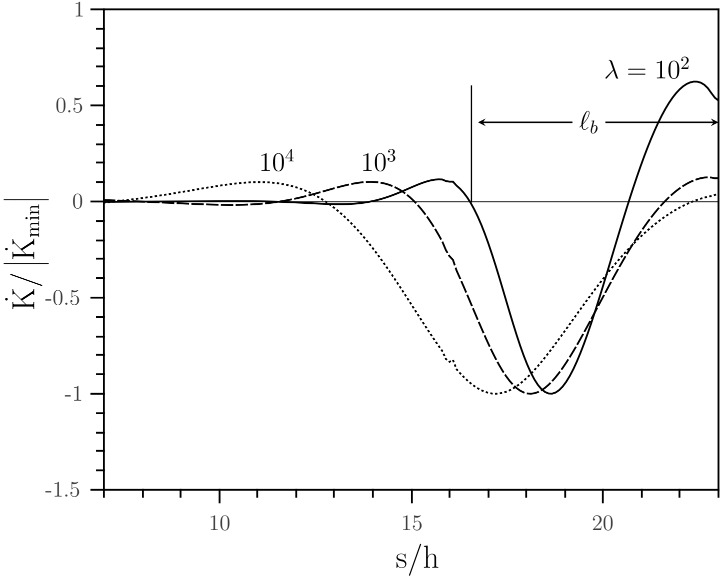

Midsurface rates of stretching (Δ), rotation (ω) and change of midsurface curvature ($\dot{K}$):

$$\Delta = U' - KW$$
$$\omega = W' + KU$$
$$\dot{K} = \omega' - K\Delta$$

Bending moment M:

$$M = -\frac{1}{3}\eta_1 h_{SP}^3 \dot{K}$$

ExtraSlide: Values of γ from other works

Table: Dimensionless interface strength of different subduction models. Asterisks indicate studies where γ has been inferred by comparison with geophysical observations.

Study	Type	γ	λ_1	Rheology
This study*	Numerical	2.0-6.3	150-450	Linear
Meyer&Schellart (2013)	Experimental	0.13-0.43	200	Linear
Duarte *et al.* (2015)*	Experimental	≤ 90	160	Linear (visco-plastic interface)
Chen *et al.* (2015)	Experimental	5.3-10.00	200	Linear (visco-plastic interface)
Holt *et al.* (2015)	Numerical	0.73-1.80	100-2000	Visco-plastic
Klein *et al.* (2015)*	Numerical (inversion from GPS data)	0.17-1.3	Elastic lithosphere	Visco-elastic asthenosphere

ExtraSlide: Rate of release of gravitational energy

Dissipation and rate of working for a volume V of fluid bounded by a surface S:

$$\underbrace{2\eta\int_V e_{ij}e_{ij}dV}_{\text{Total rate of viscous dissipation in } V} = \underbrace{\int_S u_i\hat{\sigma}_{ij}n_j dS}_{\text{Rate at which work is performed on } S \text{ by the modified stress: } \hat{\boldsymbol{\sigma}} = \boldsymbol{\sigma} + \rho g z\mathbf{I}}$$

Rate of release of gravitational energy

$$\begin{aligned} D_{\text{Total}} &= \int_{S_1} u_i(\mathbf{y})\hat{\sigma}^{(1)}_{ij}(\mathbf{y})n_j(\mathbf{y})dl(\mathbf{y}) + \int_{S_1} u_i(\mathbf{y})\hat{\sigma}^{(0)}_{ij}(\mathbf{y})\left(-n_j(\mathbf{y})\right)dl(\mathbf{y}) \\ &= \Delta\rho g\int_{S_1} u_i(\mathbf{y})n_i(\mathbf{y})y_j dl(\mathbf{y}) \quad \text{where } \mathbf{y}\in S_1 \text{ and } (\hat{\sigma}^{(1)}_{ij} - \hat{\sigma}^{(0)}_{ij})n_j = n_i\Delta\rho g y_j \end{aligned}$$

ExtraSlide: SP only case-scaling analysis

SP's portion dynamically relevant

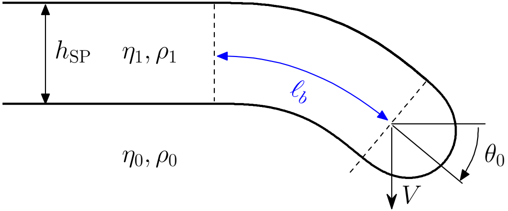

Viscous dissipation within the SP

Bending-dominated $\Rightarrow$

$$\Rightarrow D_{\mathrm{SP}} \sim \eta_1 h_{\mathrm{SP}}^3 \left(\underbrace{\frac{V}{\ell_b^2}}_{\sim \dot{K}}\right)^2 (\ell_b)\mathrm{f}_1(\theta_0)$$

Viscous dissipation within the mantle

$$D_{\mathrm{M}} \sim \eta_0 \left(\underbrace{\frac{V}{\ell_b}}_{\sim e_{ij}}\right)^2 (\underbrace{\ell_b^2}_{\sim A_{\mathrm{M}}})\mathrm{f}_2(\theta_0)$$

Dissipation ratio

$$R \sim \frac{\overbrace{\mathrm{St}}^{\text{Dynamical effect}}}{\mathrm{St} + \underbrace{\mathrm{F}(\theta_0)}_{\text{Geometrical effect}}}$$

$\Rightarrow$ Plot R vs. St for different θ_0

ExtraSlide: $D_{\mathrm{SP}}/D_{\mathrm{M}}$ overestimation

$$\alpha = (\ell_b/R_{\min})^3$$

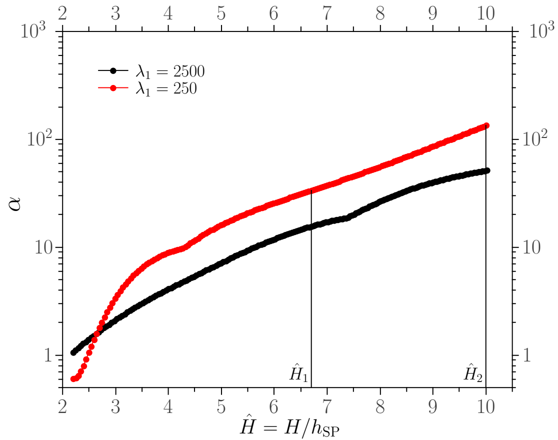

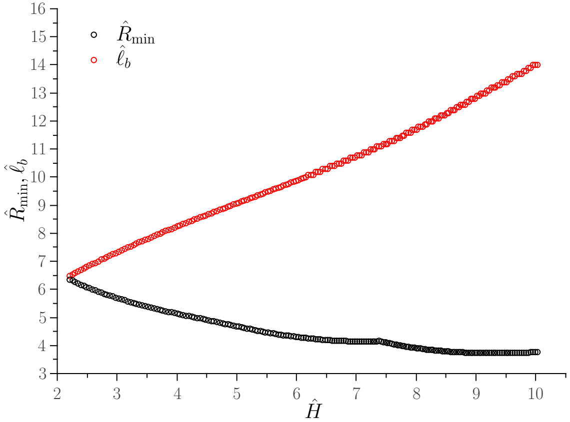

ExtraSlide: β for constant h_{SP}

$$\beta = \frac{1/2}{1 + C_{\mathrm{R}}}$$

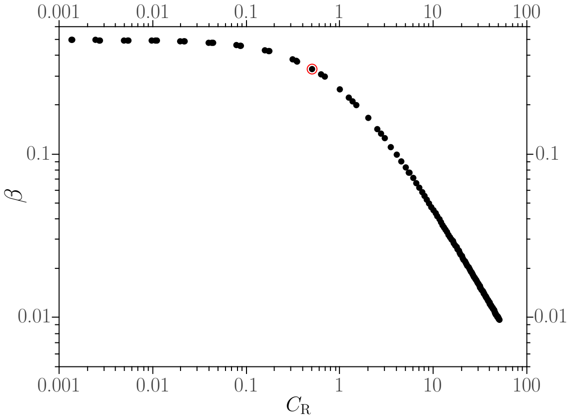

Table: Values of the energetical ratio $C_{\mathrm{R}}|_L$ and the corresponding exponent $\beta|_L$ for $L = \ell_b$ or $R_{\min}$.

$\hat{H}_1 = 6.7$	λ_1	$C_{\mathrm{R}}\|_{\ell_b}$	$C_{\mathrm{R}}\|_{R_{\min}}$	$\beta\|_{\ell_b}$	$\beta\|_{R_{\min}}$
	250	0.27	8.91	0.39	0.05
	2500	0.44	7.04	0.35	0.06
$\hat{H}_2 = 10$	λ_1	$C_{\mathrm{R}}\|_{\ell_b}$	$C_{\mathrm{R}}\|_{R_{\min}}$	$\beta\|_{\ell_b}$	$\beta\|_{R_{\min}}$
	250	0.55	73.7	0.32	≈ 0
	2500	0.60	30.6	0.31	0.02

ExtraSlide: $R_{\min}$ vs ℓ_b (Ribe, 2010)

Flexural Stiffness of the plate: $\mathrm{St} \equiv \dfrac{F_{\mathrm{int}}}{F_{\mathrm{drag}}} = \gamma \left(\dfrac{h}{L}\right)^3$

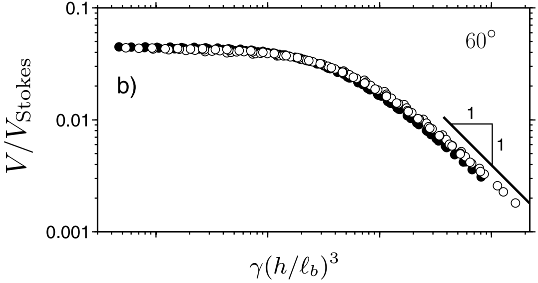

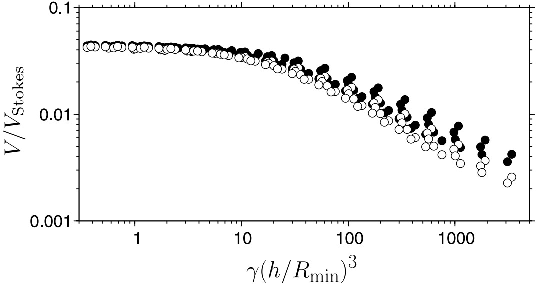

ExtraSlide: Definition C_{R} $(D_{\mathrm{SI}} = 0)$

$$C_{\mathrm{R}} \equiv \frac{R}{1-R} = \frac{D_{\mathrm{SP}}}{D_{\mathrm{M}}} = \frac{\mathrm{Ra_m}}{\mathrm{Ra_{SP}}} \mathrm{F}(\theta) \left(\frac{h_{\mathrm{SP}}}{H} \right)^3$$

BEM numerical solutions ($\lambda_1 \in [250 - 2500]$)

$$\frac{\mathrm{Ra_m}}{\mathrm{Ra_{SP}}} \in [100 - 650] \qquad \mathrm{F}(\theta) \in [0.2 - 0.8]$$

$$\frac{\mathrm{h_{SP}}}{H} = 6.7 \qquad C_{\mathrm{R}} \leq 1$$

ExtraSlide: SP ONLY case- instantaneous solutions

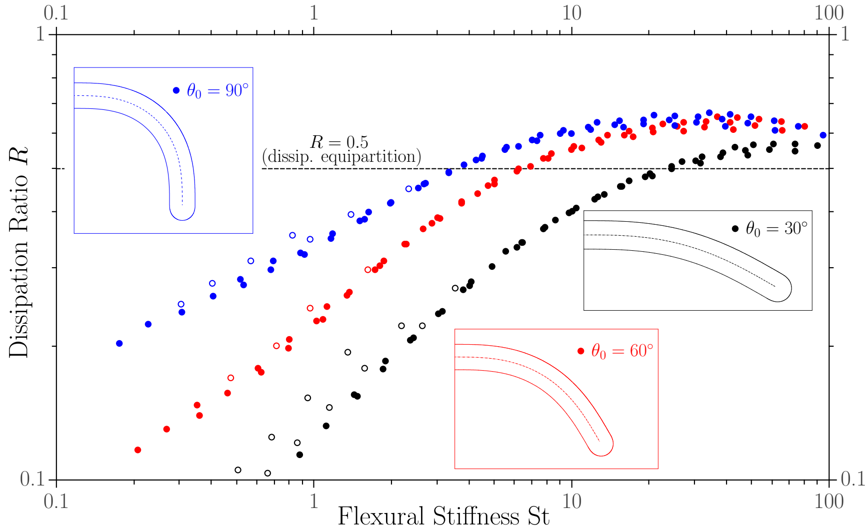

Dissipation ratio scale

Dynamical effect

$$R \sim \frac{\mathrm{St}}{\mathrm{St} + \mathrm{F}(\theta_0)}$$

Geometrical effect

Simulation parameters

$\lambda_1 = [150 - 10^5]$

$\ell / h_{\mathrm{SP}} = [5 - 10]$

$L_{\mathrm{SP}} / h_{\mathrm{SP}} = [20 - 32]$

Irrelevant

ExtraSlide: SP only case- instantaneous solutions

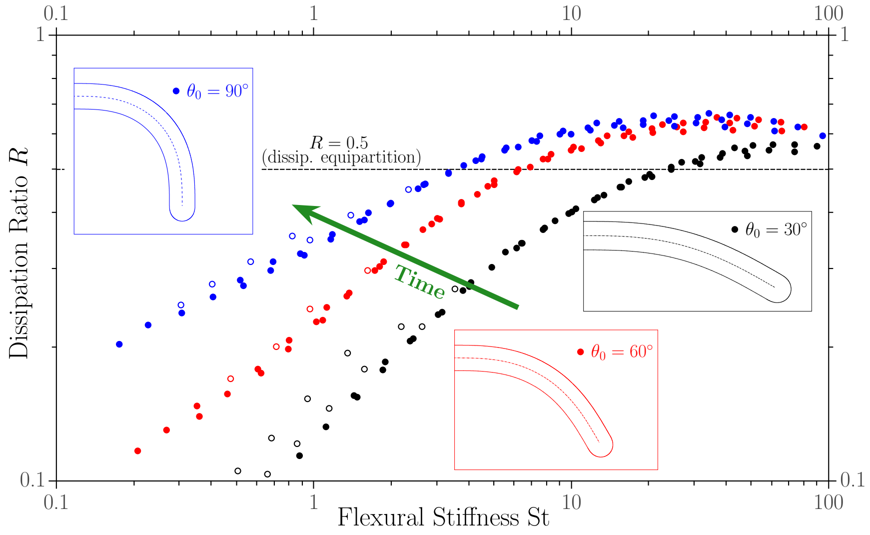

Dissipation ratio scale

Dynamical effect

$$R \sim \frac{\mathrm{St}}{\mathrm{St} + \mathrm{F}(\theta_0)}$$

Geometrical effect

Subduction Evolution

- $\mathrm{St} \downarrow \Rightarrow R \downarrow$
- $\theta \uparrow \Rightarrow R \uparrow$

Simulation parameters

$\lambda_1 = [150 - 10^5]$

$\ell / h_{\mathrm{SP}} = [5 - 10]$

$L_{\mathrm{SP}} / h_{\mathrm{SP}} = [20 - 32]$

Irrelevant

ExtraSlide: SP+OP case-instantaneous solutions

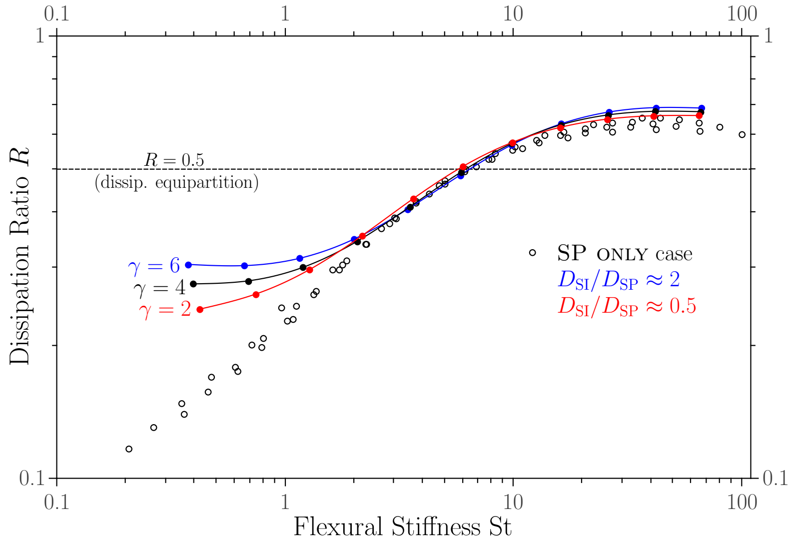

SI EFFECT

- St $\lesssim 1 \Rightarrow$ significant
- St $\gg 1 \Rightarrow$ negligible

OP DISSIPATION

$$\frac{D_{OP}}{D_{BL}} < 5\% \Rightarrow \text{negligible}$$

Steady-state analysis of thermal convection

Conrad&Hager (1999) approach: $\mathbf{Ra_{SP}} \equiv \dfrac{\ell_b^3 g \Delta\rho_1}{\kappa\eta_1}$, $\mathbf{Ra_{SI}} \equiv \dfrac{d_{SI}^3 g \Delta\rho_1}{\kappa\eta_{SI}}$

$D_{SP/SI} \gg 1 \Rightarrow \mathrm{Ra}_{SP/SI} \ll 1$

$$V_{\mathrm{Sink}} \sim \mathrm{Ra_m}\frac{h_{SP}\ell\kappa}{f_2(\theta)H^3}\left[1+\underbrace{\frac{\mathrm{Ra_m}}{\mathrm{Ra_{SP}}}\left(\frac{h_{SP}}{H}\right)^3 F(\theta)}_{\text{SP bending}}+\underbrace{\cancel{\frac{\mathrm{Ra_m}}{\mathrm{Ra_{SI}}}\left(\frac{h_{SP}}{H}\right)\left(\frac{d_{SI}^2}{H^2\sin(\theta_{SI})f_2(\theta)}\right)\left(\frac{V_{\mathrm{Conv}}}{V_{\mathrm{Sink}}}\right)^2}}_{\text{SI shearing}}\right]^{-1}$$

Strong BL ($C_R \neq 0, D_{SI} = 0$)

Thermal thickening

$$\frac{h_{SP}}{H} \sim \left(\frac{\mathrm{Ra_{SP}}}{\mathrm{Ra_m}}\frac{L_z f_2(\theta)}{\mathrm{Ra_{SP}}\ell - f_1(\theta)L_z}\right)^{1/3}$$

$$\mathrm{Nu} \sim \mathrm{Ra_m}^{1/3}\left(\frac{\ell}{L_z f_2(\theta)} - \frac{F(\theta)}{\mathrm{Ra_{SP}}}\right)^{1/3}$$

Domain of validity

$$\mathrm{Ra_{SPcr}} \rightarrow \frac{f_1(\theta)L_z}{\ell} \Rightarrow h_{SP} \rightarrow \infty \quad \mathrm{Nu} \rightarrow 0$$

BEM numerical solutions $(\lambda_1 \in [250 - 2500])$

$$\mathrm{Ra_{SPcr}} \in [3 - 10]$$

Upper mantle convection

$\mathrm{Ra_m} \in [10^5 - 10^6]$, $H/h_{SP} = 6.7$

$$D_{SP}/D_M|_{cr} \geq 7 \Rightarrow R_{cr} \approx 0.87 > [0.3 - 0.5]$$